MHD FREE CONVECTIVE SLIP FLOW OF A NANOFLUID FROM A NONLINEARLY RADIATING HEATED UPWARD FACING HORIZONTAL PLATE WITH ZERO MASS FLUX BOUNDARY CONDITION

Uddin M. J., Abelman S.* and Aphane D.
*Author for correspondence
School of Computer Science and Applied Mathematics and
DST-NRF Centre of Excellence in Mathematical and Statistical Sciences,
University of the Witwatersrand, Johannesburg,
Private Bag 3,
Wits 2050 South Africa,
E-mail: shirley.abelman@wits.ac.za

ABSTRACT

The aim of the present study is to investigate the effect of velocity slip, thermal slip and zero mass flux boundary conditions on the boundary layer flow of nanofluid over an upward facing horizontal plate. We consider two-dimensional laminar free convective boundary layer flow of a nanofluid past an upward facing permeable horizontal plate located in a porous medium. Lie group analysis is used to determine the similarity equations of the governing equations. The effects of relevant parameters on the dimensionless fluid velocity, the temperature, the nanoparticle volume fraction, the rate of heat transfer and the rate of nonoparticle volume fraction are investigated and shown graphically and discussed.

INTRODUCTION

Embedded solid-state cooling layers which have relatively high thermal conductivity in terms of the heat-generating medium into which they are introduced, present as a viable passive method of reducing peak operating temperatures in, for instance, integrated power electronic and other applications where an increase in power density is of interest. The thermal performance of such a bi-material cooling method is dependent on geometric, material property and thermal interfacial parameters. This paper reports on the influence of five such identified parameters, as obtained via a numerical study. Single-directional heat extraction from a rectangular solid-state volume is considered and the thermal performance obtained for such a boundary condition is described.

We consider two-dimensional laminar free convective boundary layer flow of a nanofluid past an upward facing permeable horizontal plate located in a porous medium. We select a coordinate frame in which the $\bar{x}$-axis is in the horizontal direction and $\bar{y}$ is normal to it, see Fig. (1). The temperature T and the nanoparticle volume fraction C assume constant values T_w and C_w, respectively at the boundary. Assume that $T_w > T_\infty$. The ambient values of T and C are denoted by T_∞ and C_∞, respectively,

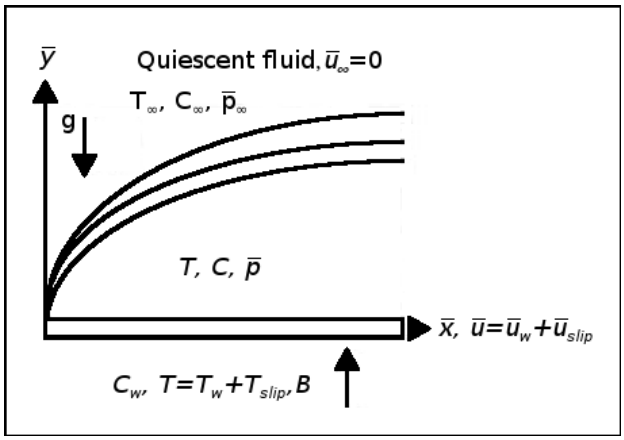

Figure 1. Coordinate system and flow model.

as y tends to infinity, . The Oberbeck-Boussinesq approximation is used. A magnetic field of variable strength is applied perpendicular to the plate. The following field equations represent the conservation of mass, momentum, thermal energy and nanoparticles, respectively. The variables are $(\bar{u},\bar{v})$: velocity components, T:the temperature and C: the nanoparticle volume fraction. Making the standard boundary layer approximation based on an order of magnitude analysis to neglect the small order terms, we have the governing equations,

$$\frac{\partial \bar{u}}{\partial \bar{x}}+\frac{\partial \bar{v}}{\partial \bar{y}}=0, \tag{1}$$

$$\rho_f\left(\bar{u}\frac{\partial \bar{u}}{\partial \bar{x}}+\bar{v}\frac{\partial \bar{u}}{\partial \bar{y}}\right)=-\frac{\partial \bar{p}}{\partial \bar{x}}+\mu\frac{\partial^2 \bar{u}}{\partial \bar{y}^2}-\frac{\sigma B_0^2}{x^{2/5}}\bar{u}, \tag{2}$$

$$\frac{\partial \bar{p}}{\partial \bar{y}}=\left[(1-C_\infty)\rho_f g\beta(T-T_\infty)-(\rho_{\bar{p}}-\rho_f)g(C-C_\infty)\right], \tag{3}$$

$$\bar{u}\frac{\partial T}{\partial \bar{x}}+\bar{v}\frac{\partial T}{\partial \bar{y}}=\alpha\frac{\partial^2 T}{\partial \bar{y}^2}+\tau\left[D_B\frac{\partial C}{\partial \bar{y}}\frac{\partial T}{\partial \bar{y}}+\left(\frac{D_T}{T_\infty}\right)\left(\frac{\partial T}{\partial \bar{y}}\right)^2\right]-\frac{1}{\rho_f c_p}\frac{\partial q_r}{\partial \bar{y}}, \tag{4}$$

$$\bar{u}\frac{\partial C}{\partial \bar{x}}+\bar{v}\frac{\partial C}{\partial \bar{y}}=D_B\frac{\partial^2 C}{\partial \bar{y}^2}+\left(\frac{D_T}{T_\infty}\right)\frac{\partial^2 T}{\partial \bar{y}^2}. \tag{5}$$

The appropriate boundary conditions are, following Karniadakis et al. [1], Kuznetsov and Nield [2], Pakravan and Yaghoubi [3]

$$\left.\begin{aligned}&\bar{u}=\lambda\bar{u_w}(\bar{x}/L)+\bar{u}_{slip},\bar{v}=0,T=T_w(\bar{x}/L)+T_{slip}(\bar{x}/L),\\&D_B\frac{\partial C}{\partial \bar{y}}+\frac{D_T}{T_\infty}\frac{\partial T}{\partial \bar{y}}=0 \text{ at } \bar{y}=0,\\&\bar{u}\to 0,T\to T_\infty,C\to C_\infty,\bar{p}\to\bar{p}_\infty \text{ as } \bar{y}\to\infty,\end{aligned}\right\} \tag{6}$$

where $\alpha=\dfrac{k}{(\rho c_{\bar{p}})_f}$ is thermal diffusivity of the fluid and $\tau=\dfrac{(\rho c_{\bar{p}})_{\bar{p}}}{(\rho c_{\bar{p}})_f}$ is a parameter, ρ_f is density of the base fluid, μ is the dynamic viscosity of the base fluid, β is the volumetric expansion coefficient of nanofluid, $\rho_{\bar{p}}$ is the density of the nanoparticles, $(\rho c_{\bar{p}})_f$ is the effective heat capacity of fluid, $(\rho c_{\bar{p}})_{\bar{p}}$ is the effective heat capacity of the nanoparticle material, k is the effective thermal conductivity of the porous medium, $\overrightarrow{g}$ is gravitational acceleration. Here D_B represents the Brownian diffusion coefficient and D_T signifies the thermophoretic diffusion coefficient, $\bar{u}_w(\bar{x}/L)=\lambda\dfrac{\alpha}{L}Ra^{2/5}\left(\dfrac{\bar{x}}{L}\right)^{1/5}$: velocity of plate, L: characteristic length of the plate, $\bar{u}_{slip}=\dfrac{\mu}{\rho}N_1(\bar{x}/L)\dfrac{\partial \bar{u}}{\partial \bar{y}}$: linear slip velocity, $N_1\left(\dfrac{\bar{x}}{L}\right)=(N_1)_0\left(\dfrac{\bar{x}}{L}\right)^{2/5}$: velocity slip factor with $(N_1)_0$ constant velocity slip factor, $T_{slip}\left(\dfrac{\bar{x}}{L}\right)=D_1(\dfrac{\bar{x}}{L})\dfrac{\partial T}{\partial \bar{y}}$: thermal slip, $D_1\left(\dfrac{\bar{x}}{L}\right)=(D_1)_0\left(\dfrac{\bar{x}}{L}\right)^{2/5}$: thermal slip factor with $(D_1)_0$ constant thermal slip factor, $\lambda>0$ is for stretching sheet, $\lambda<0$ is for shrinking sheet and $\lambda=0$ represents stationary plate. We assume that the boundary layer is optically thick and the Rosseland approximation or diffusion approximation for radiation is valid, Bég et al. [4]. Thus, the radiative heat flux for an optically thick boundary layer (with intensive absorption), as elaborated by Sparrow and Cess [5] is defined as $q_r=-\dfrac{4\sigma_1}{3k_1}\dfrac{\partial T^4}{\partial \bar{y}}$, where $\sigma_1(=5.67\times10^{-8}\dfrac{\mathrm{W}}{\mathrm{m^2K^4}})$ is the Stefan-Boltzmann constant and $k_1(\mathrm{m}^{-1})$ is the Rosseland mean absorption coefficient.
The following nondimensional variables are introduced to reduce Eqns.(1)-(6) into dimensionless form

$$\left.\begin{aligned}&x=\frac{\bar{x}}{L},y=\frac{\bar{y}}{L}Ra^{1/5},u=\frac{L}{\alpha}Ra^{-2/5}\bar{u},v=\frac{L}{\alpha}Ra^{-1/5}\bar{u},\\&\theta=\frac{T-T_\infty}{T_w-T_\infty},\phi=\frac{C-C_\infty}{C_w-C_\infty},p=\frac{L^2(\bar{p}-\bar{p}_\infty)}{\rho_f\alpha^2}Ra^{-4/5},\end{aligned}\right\} \tag{7}$$

where $Ra=g\beta(1-C_\infty)(T_w-T_\infty)L^3\rho_f/(\alpha\mu)$ is the Rayleigh number. A stream function ψ defined by

$$u=\frac{\partial \psi}{\partial y} \text{ and } v=-\frac{\partial \psi}{\partial x}, \tag{8}$$

is introduced into Eqns. (1)-(6).
Note that Eq.(1) is satisfied identically. Hence we have

$$Pr\frac{\partial^3\psi}{\partial y^3}-\frac{\partial p}{\partial x}+\frac{\partial \psi}{\partial x}\frac{\partial^2\psi}{\partial y^2}-\frac{\partial \psi}{\partial y}\frac{\partial^2\psi}{\partial y\partial x}+M\frac{1}{x^{2/5}}\frac{\partial \psi}{\partial y}=0, \tag{9}$$

$$-\frac{1}{Pr}\frac{\partial p}{\partial y}+\theta-Nr\phi=0, \tag{10}$$

$$\frac{\partial \psi}{\partial y}\frac{\partial \theta}{\partial x}-\frac{\partial \psi}{\partial x}\frac{\partial \theta}{\partial y}-\frac{\partial^2\theta}{\partial y^2}-Nb\frac{\partial \theta}{\partial y}\frac{\partial \phi}{\partial y}-Nt\left(\frac{\partial \theta}{\partial y}\right)^2+\frac{4}{3R}\frac{\partial}{\partial y}\left[\{1+(T_r-1)\theta\}^3\frac{\partial \theta}{\partial y}\right]=0, \tag{11}$$

$$Le\left[\frac{\partial \psi}{\partial y}\frac{\partial \phi}{\partial x}-\frac{\partial \psi}{\partial x}\frac{\partial \phi}{\partial y}\right]-\frac{\partial^2\phi}{\partial y^2}-\frac{Nt}{Nb}\frac{\partial^2\theta}{\partial y^2}=0. \tag{12}$$

The boundary conditions in Eq.(6) become

$$\left.\begin{aligned}&\frac{\partial \psi}{\partial x}=0,\ \frac{\partial \psi}{\partial y}=-\lambda a x^{1/5}\frac{\partial^2\psi}{\partial y^2},\ \theta=1+bx^{-2/5}\frac{\partial \theta}{\partial y},\\&Nb\phi'(0)+Nt\theta'(0)=0 \text{ at } y=0,\\&\frac{\partial \psi}{\partial y}\to 0,\ \theta\to 0,\ \phi\to 0,\ p\to 0 \text{ as } y\to\infty.\end{aligned}\right\} \tag{13}$$

The parameters in Eqns.(9)-(13) are Pr, Nt, Nb, Nr, Le, a, b, T_r, R and M. They represent the Prandtl number, the thermophoresis parameter, the Brownian motion parameter, the buoyancy ratio parameter, the Lewis number, the velocity slip parameter, thermal slip parameter, the wall temperature excess ratio parameter, the convection-radiation parameter and magnetic field parameter respectively, which are defined by Kuznetsov and Nield [2] and Uddin et al. [6; 7]

$$\left.\begin{aligned} &Pr=\frac{v}{\alpha}, \quad Le=\frac{\alpha}{D_B},\\ &Nt=\frac{\tau D_T(T_w-T_\infty)}{\alpha T_\infty}, \quad Nb=\frac{\tau D_B(C_w-C_\infty)}{\alpha},\\ &Nr=\frac{(\rho_p-\rho_f)(C_w-C_\infty)}{\rho_f\beta(1-C_\infty)(T_w-T_\infty)},\\ &a=\frac{(N_1)_0\mu Ra^{2/5}}{\rho_f L}, \quad b=\frac{(D_1)_0 Ra^{2/5}}{L},\\ &T_r=\frac{T_w}{T_\infty}, \quad R=\frac{kk_1}{4\sigma_1 T_\infty^3}, \quad M=\frac{\sigma B_0^2 L^2}{\alpha Ra^{2/5}}. \end{aligned}\right\} \tag{14}$$

SYMMETRIES OF THE PROBLEM

By applying the Lie group method to Eqns. (9)-(12), the infinitesimal generator for the problem can be written as

$$X=\xi_1\frac{\partial}{\partial x}+\xi_2\frac{\partial}{\partial y}+\eta_1\frac{\partial}{\partial\psi}+\eta_2\frac{\partial}{\partial\theta}+\eta_3\frac{\partial}{\partial\phi}+\eta_4\frac{\partial}{\partial p} \tag{15}$$

where the transformations are (x,y,ψ,θ,ϕ,p) to $(x^*,y^*,\psi^*,\theta^*,\phi^*,p^*)$.
The infinitesimals $\xi_1,\xi_2,\eta_1,\eta_2,\eta_3$ and η_4 satisfy the following first order differential equations

$$\left.\begin{aligned} &\frac{\partial x^*}{\partial\varepsilon}=\xi_1(x^*,y^*,\psi^*,\theta^*,\phi^*,p^*), \frac{\partial y^*}{\partial\varepsilon}=\xi_2(x^*,y^*,\psi^*,\theta^*,\phi^*,p^*),\\ &\frac{\partial\psi^*}{\partial\varepsilon}=\eta_1(x^*,y^*,\psi^*,\theta^*,\phi^*,p^*), \frac{\partial\theta^*}{\partial\varepsilon}=\eta_2(x^*,y^*,\psi^*,\theta^*,\phi^*,p^*),\\ &\frac{\partial\phi^*}{\partial\varepsilon}=\eta_3(x^*,y^*,\psi^*,\theta^*,\phi^*,p^*), \frac{\partial p^*}{\partial\varepsilon}=\eta_4(x^*,y^*,\psi^*,\theta^*,\phi^*,p^*). \end{aligned}\right\} \tag{16}$$

After algebraic manipulation, the forms of the infinitesimals are

$$\left.\begin{aligned} &\xi_1=c_1x+c_2, \quad \xi_2=\frac{2}{5}c_1y+c_3,\\ &\eta_1=\frac{3}{5}c_1\psi+c_4, \quad \eta_2=c_5,\\ &\eta_3=c_6, \quad \eta_4=(c_5+c_6)y+\frac{2}{5}c_1p, \end{aligned}\right\} \tag{17}$$

where $c_i(i=1,2,...,6)$ are arbitrary constants. Hence, the equations admit six finite parameter Lie group transformations. It is observed that the parameters c_2 and c_3 correspond to translations in the variables x and y, while the parameter c_4 corresponds to translation in the variable ψ. It is also observed that the parameter c_1 corresponds to scaling in the variables x, y, ψ, and p respectively. The characteristic equation is

$$\begin{aligned} \frac{\partial x}{c_1x+c_2}&=\frac{\partial y}{\frac{2}{5}c_1y+c_3}=\frac{\partial\psi}{\frac{3}{5}c_1\psi+c_4}=\dots\\ \frac{\partial\theta}{c_5}&=\frac{\partial\phi}{c_6}=\frac{\partial p}{-\alpha_2(c_5+c_6)y+\frac{2}{5}c_1p}. \end{aligned} \tag{18}$$

The similarity transformations corresponding to the characteristic equation (18) are as follows

$$\left.\begin{aligned} &\eta=\frac{y}{x^{2/5}}, \quad \psi=x^{3/5}f(\eta), \quad p=x^{2/5}h(\eta),\\ &\theta=\theta(\eta), \quad \phi=\phi(\eta) \end{aligned}\right\} \tag{19}$$

For simplicity we assume that $c_i=0,(i=3,...,6)$

SIMILARITY EQUATIONS

On substituting the transformations in Eq.(19) into the governing Eqs.(9)-(13), we obtain the following similarity equations:

$$Pr\,f'''+\frac{3}{5}ff''-\frac{1}{5}f'^2+\frac{2}{5}\eta h'-\frac{2}{5}h-Mf'=0, \tag{20}$$

$$-\frac{1}{Pr}h'+\theta-Nr\phi=0, \tag{21}$$

$$\theta''+\frac{3}{5}f\theta'+Nb\,\theta'\phi'+Nt\,\theta'^2+\frac{4}{3R}\left[\{1+(T_r-1)\theta\}^3\theta'\right]'=0, \tag{22}$$

$$\phi''+\frac{3}{5}Le\,f\phi'+\frac{Nt}{Nb}\theta''=0, \tag{23}$$

whether $'=\frac{d}{d\eta}$, subject to the following boundary conditions,

$$\left.\begin{aligned} &f(0)=0, \quad f'(0)=\lambda+af''(0),\\ &\theta(0)=1+b\theta'(0), \quad Nb\phi'(0)+Nt\theta'(0)=0,\\ &f'(\infty)=\theta(\infty)=\phi(\infty)=h(\infty)=0. \end{aligned}\right\} \tag{24}$$

DERIVATION OF NUMERICAL SCHEME

In order to determine solutions to Eqns. (20)-(23), we convert Eqns. (20)-(23) into a system of first order ordinary differential equations by letting $f=y_1$, $f'=y_2$,...., $\theta=y_6$, $\theta'=y_7$ and substituting for the respective functions and derivatives in the original Eqns. (20)-(23). After some algebraic manipulation the resulting system of first order ordinary differential equations is

$$\left.\begin{aligned} &f=y_1, \quad f'=y_2, \quad f''=y_3,\\ &f'''=\frac{1}{5Pr}\left(-3y_1y_3+y_2^2-2\eta Pr[y_6-Nry_4]+5My_2\right), \end{aligned}\right\} \tag{25}$$

$$\left.\begin{aligned} &\phi = y_4, \quad \phi' = y_5 \\ &\phi'' = -\frac{3}{5}Le y_1 y_5 - \frac{Nt}{Nb}[\theta''] \end{aligned}\right\} \tag{26}$$

$$\left.\begin{aligned} &\theta = y_6, \quad \theta' = y_7 \\ &\theta'' = \frac{-\frac{3}{5}y_1 y_7 - Nb y_7 y_5 - Nt y_7^2 - \frac{4}{R}\left[(1+(T_r-1)y_6))^2 (T_r-1)y_7^2\right]}{\left[1+\frac{4}{3R}(1+(T_r-1)y_6)^3\right]}. \end{aligned}\right\} \tag{27}$$

Now that we have our numerical scheme (25)-(27) we can solve the system numerically using Matlab. Before any computations can occur we must restrict our domain to η and parameter values for which Eqn. (25)-(27) would have undefined values. The domain is orignally defined from 0 to ∞, but from the physical system we know that $\eta \leq 5$ will suffice. Parameter values for which Eqn. (25)-(27) will have undefined values are $P = 0$, $Nb = 0$, $R = 0$ and $Tr = 1$.

COMPARISONS

It is worth mentioning that in the case of hydrodynamic boundary layer flow past a non-radiating stationary plate with no slip boundary conditions at the wall ($M = a = b = \lambda = 0$), the problem reduces to that which has recently been investigated by Pradhan et al. [8].

PHYSICAL QUANTITIES

The parameters of engineering interest are the local skin friction factor $C_{f\bar{x}}$, the local Nusselt number $Nu_{\bar{x}}$ respectively. Physically, $C_{f\bar{x}}$ indicates wall shear stress, $Nu_{\bar{x}}$ indicates the rate of heat transfer. These quantities can be calculated from the following relations:

$$C_{f\bar{x}} = \frac{2\mu}{\rho U_r^2}\left(\frac{\partial \bar{u}}{\partial \bar{y}}\right)_{\bar{y}=0}, \quad Nu_{\bar{x}} = \frac{-\bar{x}}{T_w - T_\infty}\left(\frac{\partial T}{\partial \bar{y}}\right)_{\bar{y}=0}. \tag{28}$$

Here $U_r = g\beta(1-C_\infty)(T_w - T_\infty)\dfrac{L^2}{\alpha}$ is the characterictic velocity. By substituting from Eqns.(7) and (19) into Eq.(28), we obtain

$$\left.\begin{aligned} &Ra_{\bar{x}}^{7/5} Pr C_{f\bar{x}} = f''(0), \\ &Ra_{\bar{x}}^{-1/5} Nu_{\bar{x}} = -\left[1+\frac{4}{3R}\{1+(T_r-1)\theta(0)\}^3\right]\theta'(0). \end{aligned}\right\} \tag{29}$$

Here $Ra_{\bar{x}} = g\beta(1-C_\infty)\Delta T \bar{x}^3/(\alpha\nu)$ is the local Rayleigh number. Due to zero mass flux boundary conditions, no mass flux exists at the boundary.

RESULTS AND DISCUSSION

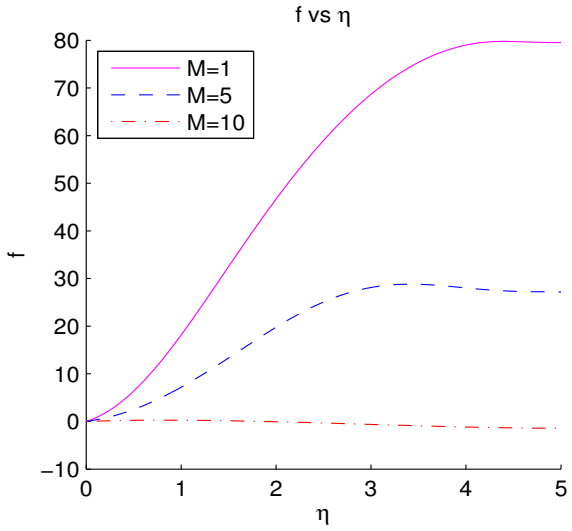

Figure 2. Effect of parameter M on f.

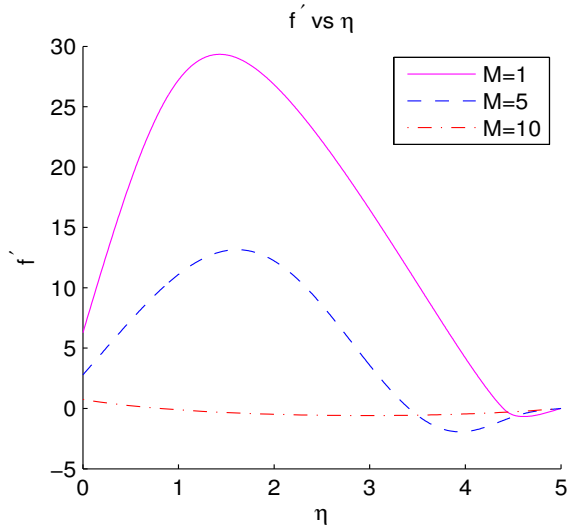

Figure 3. Effect of parameter M on f'.

Parameter values $\lambda = 1$, Le=10, Pr=6.8, a=0.2, b=0.1, Nr=0.2, Nb=0.6, Nt=0.1, Tr=1.2 and$R$=1 were used to plot Figs. 2 and 3. We observe that as M increases, both f and f' decrease. f' has turning points on the graphs for $M = 1$ and $M = 5$. For $M = 1$ and $M = 5$,f' reaches a maximum value at about $\eta = 1.5$ and then starts decreasing. For $M = 10$, both f and f'remain virtually equal to zero.

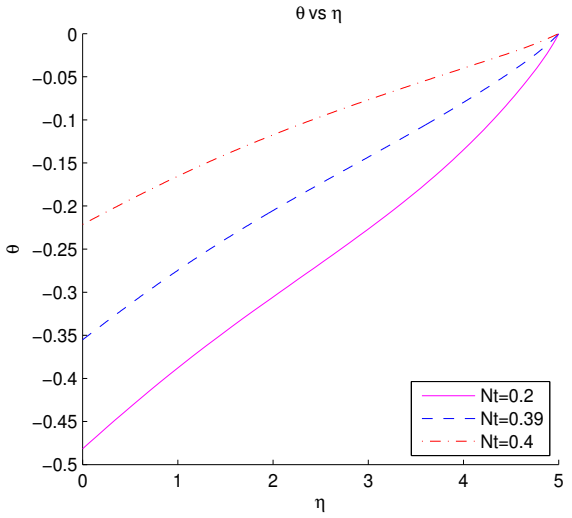

Figure 4. Effect of parameter *Nt* on θ.

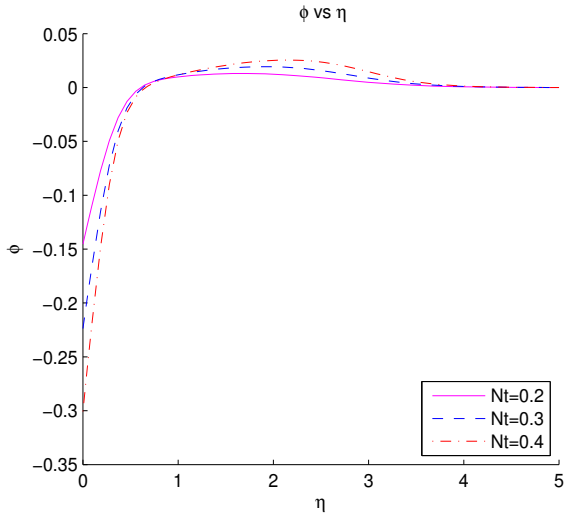

Figure 6. Effect of parameter *Nt* on θ.

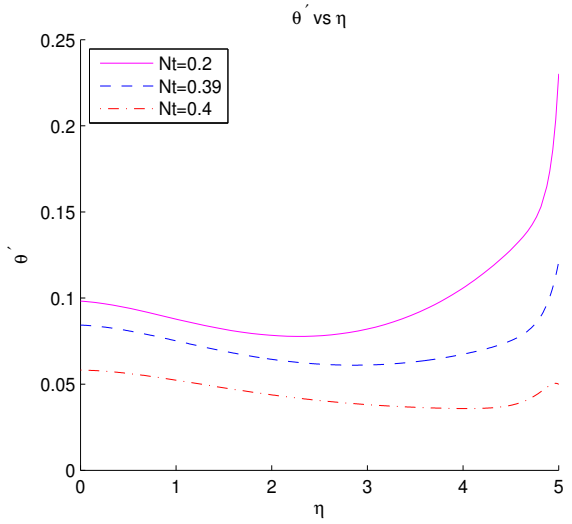

Figure 5. Effect of parameter *Nt* on θ′.

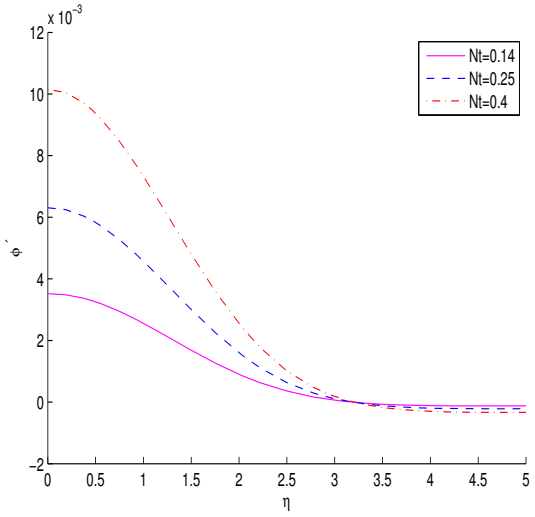

Figure 7. Effect of parameter *Nt* on θ′.

Parameter values $\lambda = 1$, *Le*=10, *Pr*=6.8, *a*=0.2, *b*=0.1, *Nr*=0.2, *M*=1, *Nb*=0.9, *Tr*=1.2 and *R*=1 were used to plot Figs. 4 and 5. We observe that as *Nt* increases, θ increases very slowly to reach zero, while θ′ decreases as *Nt* increases. A steady increase in θ′ is observed at approximately $\eta = 3.5$ when $Nt = 0.2$ and at approximately $\eta = 4.5$ when $Nt = 0.39$ and 0.4.

Parameter values $\lambda = 1$, *Le*=10, *Pr*=6.8, *a*=0.6, *b*=0.6, *Nr*=0.2, *M*=1, *Nb*=1, *Tr*=1.1 and *R*=1 were used to plot Fig. 6, while for 7 parameter values $\lambda = 1$, *Le*=10, *Pr*=6.8, *a*=15, *b*=10, *Nr*=0.9, *M*=10, *Nb*=4, *Tr*=1.1 and *R=1.5* were used. As *Nt* increases, ϕ decreases for $\eta \leq 1$. For $\eta > 1$, ϕ begins to increase as *Nt* increases. As *Nt* decreases, ϕ′ decreases. As η increases from 0 to 5, ϕ′ decreases rapidly converging to $\phi' = 0$. The boundary layer thickness is largest for Brownian parameter *Nt* = 0.4.

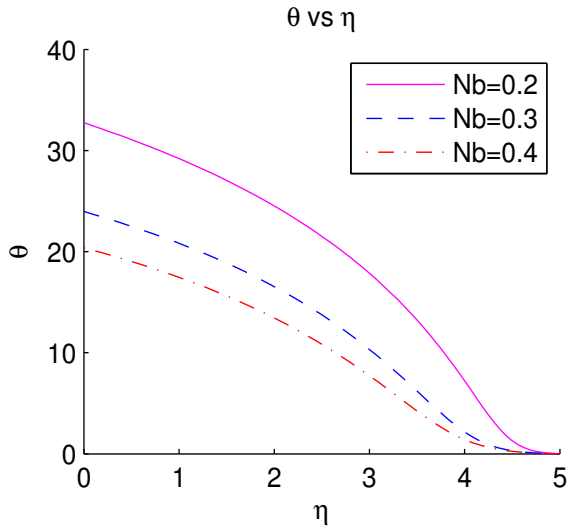

Figure 8. Effect of parameter *Nb* on θ.

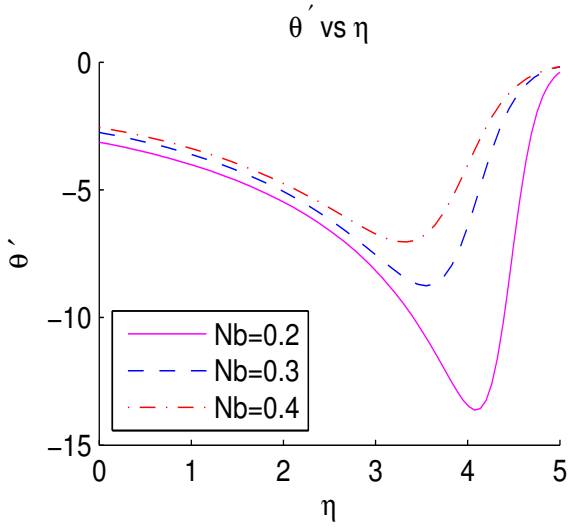

Figure 9. Effect of parameter *Nb* on θ′.

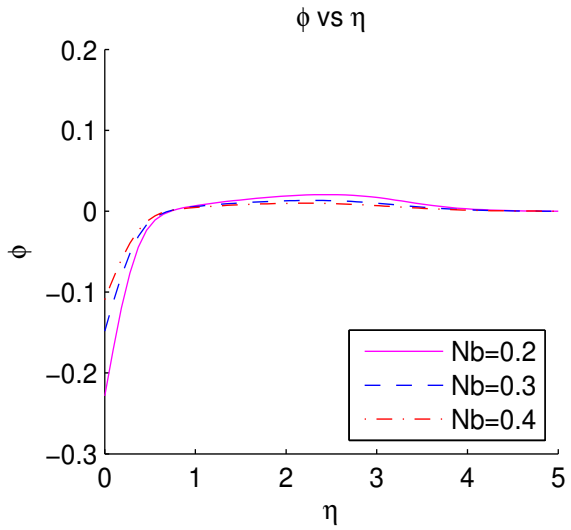

Figure 10. Effect of parameter *Nb* on ϕ.

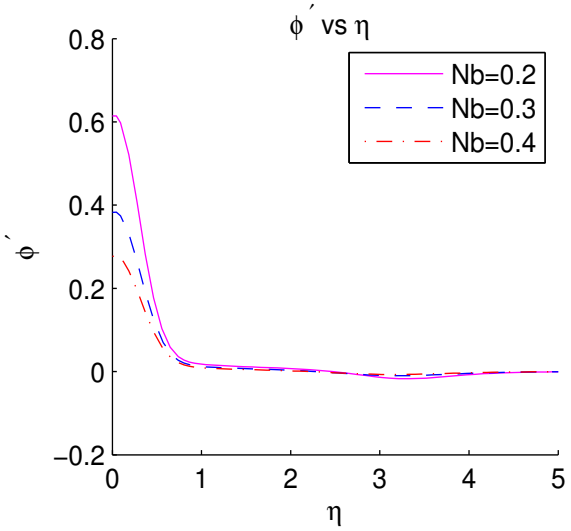

Figure 11. Effect of parameter *Nb* on ϕ′.

Parameter values $\lambda = 1$, *Le*=10, *Pr*=6.8, *a*=0.2, *b*=0.5, *Nr*=0.3, *M*=10, *Nt*=0.1, *Tr*=1.1 and *R*=1 were used to plot Figs. 8 and 9. As *Nb* increases, θ decreases eventually converging to zero at $\eta = 5$. As *Nb* decreases, θ′ decreases. We observe that each θ′-curve has a turning point for the corresponding value of *Nb*. The turning point corresponding to *Nb* = 0.2 occurs at approximately $\eta = 4$, while the turning points corresponding to *Nb* = 0.3 and 0.4 occur at approximately $\eta = 3.5$. As *Nb* increases the turning point moves upwards to the left.

Parameter values $\lambda = 1$, *Le*=10, *Pr*=6.8, *a*=0.7, *b*=1, *Nr*=0.2, *M*=1, *Nt*=0.1, *Tr*=1.2 and *R*=1 were used to plot Figs. 10 and 11. As *Nb* increases, ϕ increases for $\eta < 1$. For $\eta \in (1,5)$, ϕ decreases rapidly to zero as *Nb* increases. As *Nb* increases, ϕ′ decreases for $\eta \leq 1$. For $\eta > 1$, $\phi' \to 0$, for each value of *Nb*.

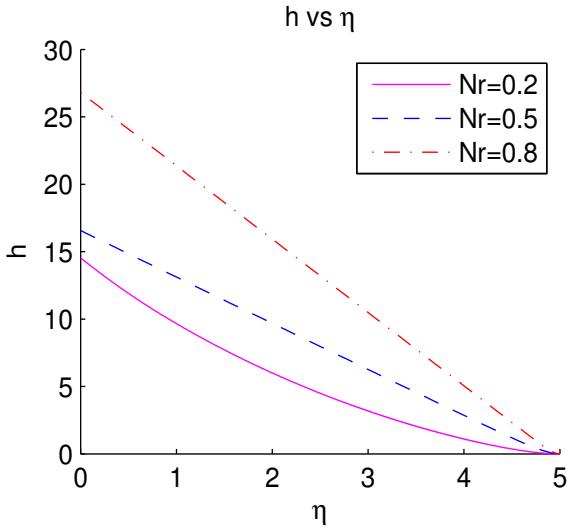

Figure 12. Effect of parameter Nr on h.

Parameter values $\lambda = 1$, Le=10, Pr=6.8, a=0.4, b=0.1, Nt=0.37,M=5.1, Nb=0.1, Tr=1.2 and R=1 were used to plot Fig. 12. As the buoyancy ratio parameter Nr decreases, h decreases. h is a decreasing function of η. As Nr decreases $h \to 0$ as $\eta \to \infty$.

CONCLUSIONS

We performed a numerical study for 2-D steady laminar incompressible boundary layer flow of a nanofluid over an upward facing horizontal permeable plate in a porous medium considering the thermal convective boundary condition. The governing boundary layer equations were transformed into highly nonlinear coupled ordinary differential equations using Lie group analysis, and then solving these equations numerically using Matlab. The following conclusions may be drawn from this research:

From Fig. (2) the fluid velocity f decreased as we increased the magnetic field parameter M. From Fig. (3) f' decreased as we increased the value of M. We see that M = 10 has virtually no influence on the behavior of f' as it remains virtually constant equal to zero. From Fig. (4) the temperature increased as the thermophoresis parameter Nt increased. From Fig. (5), θ' initially decreased with increasing values of Nt. At approximately $\eta = 4$ an increase in θ' is observed for increasing values of Nt. From Fig. (6) the nanoparticle volume fraction ϕ initially decreased, as we increased the thermophoresis parameter Nt. From Fig. (7) ϕ' decreased with decreasing Nt eventually tending to zero as $\eta \to \infty$. From Fig. (8) the temperature θ decreases as Nb increased, while from Fig. (9) θ' decreased with decreasing values of Nb. From Fig. (10) the nanoparticle volume fraction ϕ initially increased, as we increased the Brownian motion parameter Nb. However at approximately $\eta = 1$, $\phi \to 0$. From Fig. (11) ϕ' decreased with increasing Nb eventually tending to zero as $\eta \to \infty$. From Fig. (12) as the buoyancy ratio parameter Nr decreased, h is a decreasing function of η, with $h \to 0$ as $\eta \to \infty$.

ACKNOWLEDGMENT

The reviewers are thanked for their careful reading of the manuscript. Their comments have resulted in a much improved paper.

REFERENCES

[1] Karniadakis G., Beskok A., and Aluru N., Microflows and nanoflows: Fundamentals and simulation, *Springer*, *Verlag-New York*, 2005, Chaps. 5

[2] Kuznetsov A.V., and Nield D.A., Natural convective boundary-layer flow of a nanofluid past a vertical plate: A revised model, *International Journal of Thermal Sciences*, Vol. 77, 2014, pp. 126-129

[3] Pakravan H., and Yaghoubi M., Analysis of nanoparticles migration on natural convective heat transfer of nanofluids, *International Journal of Thermal Sciences*, Vol. 68, 2013, pp. 78-93

[4] Bég O.A., Zueco J., Bég T.A., Takhar H. S., and E. Kahya, NSM analysis of time-dependent nonlinear buoyancy-driven double-diffusive radiative convection flow in non-Darcy geological porous media,*Acta Mechanica*, vol. 202, 2009, pp. 181204

[5] Sparrow E. M., and Cess R.D., Radiation Heat Transfer, *Hemisphere*, *Washingtion*, 1978, Chaps. 7 & 10

[6] Uddin M.J., Khan W.A., and Ismail A.I., Lie Group Analysis of Natural Convective Flow from a Convectively Heated Upward Facing Radiating Permeable Horizontal Plate in Porous Media Filled with Nanofluid, *Journal of Applied Mathematics* Vol. 2012, 2012, Article ID 648675

[7] Uddin M.J., Bég O.A., and Amin N., Hydromagnetic transport phenomena from a stretching or shrinking nonlinear nanomaterial sheet with Navier slip and convective heating: A model for bio-nano-materials processing, *Journal of Magnetism and Magnetic Materials*, Vol. 368, 2014, pp. 252-261

[8] Pradhan K, Samanta S., and Guha A., Natural Convective Boundary Layer flow of Nanofluids Above an Isothermal Horizontal Plate, *Journal of Heat Transfer*, Vol. 136, 2014, pp. 102501(8pages)